A comprehensive study on the internal structure and thedensity distribution of ^{12}Be

M. Aygun
Department of Physics, Bitlis Eren University, Bitlis, Turkey.

Received 24 November 2015; accepted 8 April 2016

In this study, a comprehensive investigation on both different internal structure dynamics and various density distributions of the ^{12}Be nucleus is conducted. With this goal, the quasielastic scattering data of the ^{12}Be + ^{12}C reaction is analyzed. Firstly, six different density distributions of the ^{12}Be nucleus are used to obtain the real potentials under the double folding model. The imaginary potentials in the calculations of all the density distributions are taken as Woods-Saxon type. The obtained theoretical results are compared with the literature results as well as the experimental data. This comparison provides information about the similarities and differences of the six different density distributions used in the calculations. Finally, by using a different method, various internal structure models of the ^{12}Be nucleus which consist of the ^{4}He + ^{8}He, ^{6}He + ^{6}He and ^{4}He + ^{6}He + 2n systems are investigated. The theoretical results are given in comparison with each other as well as the experimental data. The agreement with the data of the theoretical results is very good.

Keywords: Optical model; elastic scattering.

PACS: 24.10.Ht; 24.50.+g; 25.70.-z

1. Introduction

Be isotopes have attracted much interest in the field of nuclear physics. These nuclei have been considered in different forms. For example, ^{11}Be which has a low binding energy for the last neutron and a large radius in proportion to ^{10}Be is called one neutron halo nucleus (^{10}Be + n). ^{13}Be is not bound. ^{14}Be has often been assumed to occur in a three-body system with ^{12}Be + n + n. In addition to this, ^{14}Be can be considered as a five-body system with ^{10}Be + n + n + n + n. ^{12}Be is one of the most interesting of Be isotopes. The binding energy of ^{12}Be is 3.67 MeV. The ^{12}Be nucleus demonstrates the cluster structure and has an important effect in the vanishing of the neutron magic number $N = 8$ [1]. Therefore, the experimental and theoretical studies on the ^{12}Be nucleus still continue [2–8].

When explaining the experimental data of stable nuclei, a Woods-Saxon type density distribution or a Fermi type density distribution or a harmonic-oscillator type density distribution has been extensively used. [9, 10]. On the other hand, the density distributions of halo nuclei present a long tail. Also, the cross-section of nucleus-nucleus scattering is sensitive to the density distribution used [11, 12]. Henceforth, it is important to examine the density distributions of nuclei. In this context, different density distributions for ^{12}Be isotope have been proposed. These density distributions are the Variational Monte Carlo (VMC), the Single-Gaussian (SG), Gaussian-Gaussian (GG), Gaussian-Halo (GH), Gaussian-Oscillator (GO), and Gaussian-Exponential (GE) density distributions. We consider that a comparative analysis of these density distributions would be useful in the analysis of the reactions with ^{12}Be. In our work, it is chosen ^{12}Be + ^{12}C system. Zahar *et al.* [13] measured quasielastic scattering of the ^{12}Be + ^{12}C system at 679 MeV. They carried out the phenomenological calculations within the optical model (OM) and inelastic scattering for the 2^+ excited state of ^{12}C nucleus in the coupled-channels (CC) formalism in order to explain the experimental data. They showed that it is convenient to use a potential with a much deeper surface imaginary component and an attractive surface real component in obtaining good agreement results with the experimental data of the ^{12}Be + ^{12}C system. Mermaz [14] performed a theoretical analysis for quasielastic scattering of the ^{12}Be + ^{12}C system under the same energy and conducted the OM calculations with volume Woods-Saxon (WS) type plus surface terms for real and imaginary potentials. Although the phenomenological approach within the framework of the OM has been generally used in these studies, a microscopic approach such as the double folding model (DFM) has not been applied to the analysis of this reaction. The DFM together with the density distributions of both projectile nucleus and target nucleus [15] is used to obtain the real part of the optical potential. The DFM has been applied extensively in the theoretical analysis of the elastic scattering interactions for various nuclear systems [16–23]. Therefore, we intend to investigate the quasielastic scattering of ^{12}Be on ^{12}C by using the VMC, SG, GG, GH, GO and GE density distributions existing in the literature via the DFM.

Cluster structures are an important tool to investigate the structure of a nucleus and to constitute different configurations with elements and to understand the processes in nuclear astrophysics [24, 25]. Neutron-rich Be isotopes are thought to be an important candidate for the cluster studies [26,27]. In this context, the structural differences between the studies performed on the ^{12}Be nucleus, where the neutron magic number $N = 8$ was noticed to have broken down, and molecular or cluster states for ^{12}Be nucleus were observed. The ground state of ^{12}Be is not considered as a halo candidate [28]. It should not be supposed that the ^{12}Be nucleus is well defined with 2n and inert-core model if the core is in the

^{10}Be form [28]. Therefore, different structures could be considered for the ^{12}Be nucleus such as ^{4}He + ^{8}He, ^{6}He + ^{6}He and ^{4}He + ^{6}He + 2n [25, 29]. As a result of this, both experimental and the theoretical studies began to get involved in these cases [30–33]. It has been reported that ^{12}Be levels can decay through ^{6}He + ^{6}He and α + ^{6}He exit channels [34–36]. Saito *et al.* [37] showed the existence of ^{6}He + ^{6}He breakup states. Descouvemont and Baye [38] reported that the molecular states of ^{12}Be can be a mixing of ^{6}He + ^{6}He and α + ^{8}He configurations. Nevertheless, the studies on this case of ^{12}Be still continue. Thus, to examine the role of the core and valence for ^{12}Be will be very useful and interesting during the analysis of the reactions with ^{12}Be. With this goal, we plan to investigate each one of these configurations of the ^{12}Be nucleus within the DFM.

The theoretical calculations of the present study fall into two categories. Firstly, we focus on the analysis of the ^{12}Be + ^{12}C system for six type density distributions of the ^{12}Be nucleus by using the DFM based on the OM. We obtain the scattering angular distributions for all different density distributions. We compare the theoretical results with the experimental data and the literature results. Finally, we investigate the ^{4}He + ^{8}He, ^{6}He + ^{6}He and ^{4}He + ^{6}He + 2n models for the ^{12}Be nucleus by using the DFM. We acquire the elastic scattering angular distribution for each of these systems. We compare the theoretical results with the experimental data.

In the next section, we demonstrate the OM calculations. In Sec. 3, we define all the densities used in the present study. In Sec. 4, the parametrization of the internal structure models of the ^{12}Be nucleus is shown. In Sec. 5, the results of these calculations are given. Section 6 is devoted to our summary and conclusion.

2. Optical model calculations

To determine the real part of nuclear potential is applied the DFM which uses the nuclear matter distributions of both the projectile and target nucleus together with an effective nucleon-nucleon interaction potential (ν_{NN}). The double folding potential is

$$V_{\text{double folding}}(\mathbf{r}) = \int d\mathbf{r_1} \int d\mathbf{r_2} \rho_P(\mathbf{r_1}) \rho_T(\mathbf{r_2}) \nu_{NN}(r_{12}), \quad (1)$$

where $\rho_P(\mathbf{r}_1)$ and $\rho_T(\mathbf{r}_2)$ are the nuclear matter densities of projectile and target nuclei, respectively. In order to make a comparative study, we have used various density distributions for the ^{12}Be nucleus. Each of these densities is explained in the following. The density of the ^{12}C target nucleus is taken as below

$$\rho_{^{12}C}(r_2) = \rho_0 \, (1 + w r_2^2) \, \exp\,(-\beta r_2^2), \quad (2)$$

where ρ_0 = 0.1644 fm^{-3}, w = 0.4988 fm^{-2}, and $\beta = 0.3741$ fm^{-2} [39, 40].

In our study, we have used the most common one, the M3Y nucleon-nucleon (Michigan 3 Yukawa) realistic interaction, which is given by

$$\nu_{NN}(r) = 7999 \frac{\exp(-4r)}{4r} - 2134 \frac{\exp(-2.5r)}{2.5r} + J_{00}(E)\delta(r)\,, \quad (3)$$

where $J_{00}(E)$ is the exchange term in the following form

$$J_{00}(E) = \, 276 \, [1 - 0.005 \, E_{\text{Lab}}/A_p]. \quad (4)$$

Finally, the imaginary potential is taken in the WS form

$$W(r) = W_0/(1 + e^x), \qquad x = (r - R_w)/a_w \quad (5)$$

where $R_w = r_w \, (A_P^{1/3} + A_T^{1/3})$ and A_P and A_T are mass numbers of projectile and target nuclei, respectively. Here, W_0, r_w and a_w parameters, respectively are the depth, the radius and the diffuseness of the imaginary part of optical potential.

3. Parametrization of density distributions

In our work, we have used six kind densities of the ^{12}Be nucleus to generate the real part used in explaining of the scattering cross-section of ^{12}Be by ^{12}C. These density distributions are the VMC, SG, GG, GH, GO, and GE densities.

3.1. The Variational Monte Carlo (VMC) density distribution

The Variational Monte Carlo (VMC) method is applied to construct a variational wave function. The density distribution of the ^{12}Be nucleus obtained from the VMC calculations using the Argonne v18 (AV18) two-nucleon and Urbana X three-nucleon potentials (AV18+UX) has been reported [41].

3.2. The Single-Gaussian (SG) density distribution

The point nucleon density of the nucleus examined via the SG density distribution is determined by using the following equation [42]

$$\rho(r) = \left(\frac{3}{2\pi R_m^2}\right)^{3/2} \exp\left(-\frac{3r^2}{2R_m^2}\right), \quad (6)$$

where R_m is the root mean square (rms) matter radius of the nucleus. In our calculations, the value of R_m is taken as 2.580 fm [43].

3.3. The Gaussian-Gaussian (GG) density distribution

If the investigated nucleus consists of a core (^{10}Be) and valence neutrons (2n), the core and the valence density distributions of this nucleus can be taken as [44]

$$\rho_c(r) = \left(\frac{3}{2\pi R_c^2}\right)^{3/2} \exp\left(-\frac{3r^2}{2R_c^2}\right) \quad (7)$$

$$\rho_v(r) = \left(\frac{3}{2\pi R_v^2}\right)^{3/2} \exp\left(-\frac{3r^2}{2R_v^2}\right), \quad (8)$$

where R_c and R_v are the rms radii of the core and valence nucleon distributions, respectively. The total matter distribution ρ_m is given in following form

$$\rho_m(r) = [N_c\rho_c(r) + (A - N_c)\rho_v(r)]/A, \quad (9)$$

where N_c is the number of nucleons in the core and A is mass number. In our calculations, the values of R_c and R_v are 2.39 fm and 4.02 fm, respectively [43]. For these values, we found R_m=2.730 fm.

3.4. The Gaussian-Halo (GH) density distribution

The GH density is expressed by

$$\rho_m(r) = \left(\frac{3}{2\pi R_m^2}\right)^{3/2} [1 + \alpha\varphi(r)] \exp\left(-\frac{3r^2}{2R_m^2}\right), \quad (10)$$

where

$$\varphi(r) = \frac{3}{4}\left[5 - 10\left(\frac{r}{R_m}\right)^2 + 3\left(\frac{r}{R_m}\right)^4\right]. \quad (11)$$

α is a parameter in the range 0$\leq \alpha \leq$ 0.4. For α=0, the GH density satisfies the gaussian function, whereas the values close to 0.4 of the α give a density distribution with the halo component. While the GH density distribution is obtained, the values of R_m and α are taken as 2.68 fm and 0.08 fm, respectively [43]. Thus, the R_m is 2.679 fm.

3.5. The Gaussian-Oscillator (GO) density distribution

For determining this kind of the density distribution, we assume that the ^{12}Be density is the sum of the core (^{10}Be) and valence (2n) densities. In this context, the core density is evaluated as

$$\rho_c(r) = \left(\frac{3}{2\pi R_c^2}\right)^{3/2} \exp\left(-\frac{3r^2}{2R_c^2}\right). \quad (12)$$

The 1p-shell harmonic oscillator density is applied to generate the valence density distribution. It is formulated by

$$\rho_v(r) = \frac{5}{3}\left(\frac{5}{2\pi R_v^2}\right)^{3/2} \left(\frac{r}{R_v}\right)^2 \exp\left(-\frac{5r^2}{2R_v^2}\right). \quad (13)$$

The ρ_m is written as

$$\rho_m(r) = [N_c\rho_c(r) + (A - N_c)\rho_v(r)]/A \quad (14)$$

In our study, the values of R_c and R_v are 2.33 fm and 4.08 fm, respectively [43]. For these values, we obtained R_m=2.575 fm.

3.6. The Gaussian-Exponential (GE) density distribution

Finally, we assume that the ^{12}Be density consists of the sum of the core (^{10}Be) and valence (2n) densities. The core density is parameterized as

$$\rho_c(r) = \left(\frac{3}{2\pi R_c^2}\right)^{3/2} \exp\left(-\frac{3r^2}{2R_c^2}\right). \quad (15)$$

The exponential density of the valence is given by

$$\rho_v(r) = \frac{r^2}{R_v^5} \exp\left(-\sqrt{30}\frac{r}{R_v}\right). \quad (16)$$

In our calculations, R_c and R_v are 2.20 fm and 5.75 fm, respectively [42]. The value of R_m has been found as 2.275 fm.

4. Parametrization of internal structure models of the ^{12}Be nucleus

Here, we examine the internal structure of the ^{12}Be nucleus by using a new approach. When the ^{12}Be nucleus is handled in a theoretical manner, different structures of ^{12}Be can be taken into account. The structures investigated in this work consist of the ^{4}He + ^{8}He, ^{6}He + ^{6}He and ^{4}He + ^{6}He + 2n systems.

4.1. The ^{4}He + ^{8}He system

It is assumed that the ^{12}Be nucleus consists of the ^{4}He + ^{8}He model. Thus, the ^{12}Be density is the sum of the densities of the ^{4}He and ^{8}He nuclei formulated in the following

$$\rho_{^{12}Be}(r) = \rho_{^4He}(r) + \rho_{^8He}(r). \quad (17)$$

The density of the ^{4}He nucleus is taken as [15]

$$\rho_{^4He}(r) = 0.4229 \ \exp(-0.7024r^2). \quad (18)$$

For this density distribution, the neutron and proton densities have assumed the same radial shape. The ^{8}He density, which is considered to be the sum of the core and valance densities, is given in the following formulas [45]

$$\rho_c(r) = \frac{1}{\pi}\frac{2}{\sqrt{\pi}}\frac{1}{a^3} \ \exp\left(\frac{-r^2}{2a^2}\right) \qquad \text{where}$$
$$a = \frac{1.69}{\sqrt{3}} \ \text{fm}, \quad (19)$$

and

$$\rho_v(r) = \frac{8}{3\pi\sqrt{\pi}}\frac{r^2}{b^5} \ \exp\left(\frac{-r^2}{b^2}\right), \qquad \text{where}$$
$$b = 1.99 \ \text{fm}, \quad (20)$$

where $\rho_c(r)$ and $\rho_v(r)$ are the core and valence density distributions, respectively.

4.2. The ^{6}He + ^{6}He system

Also, the ^{12}Be nucleus can be handled as the ^{6}He + ^{6}He system. Thus, the ^{12}Be density is the sum of the the density distributions of the ^{6}He exotic nuclei written as

$$\rho_{^{12}Be}(r) = \rho_{^6He}(r) + \rho_{^6He}(r). \quad (21)$$

We have used two different density distributions for the ^{6}He nucleus in our calculations. The first density distribution of ^{6}He is No-Core Shell-Model (NCSM), which is taken from [46]. The second density of ^{6}He is formulated by

$$\rho_{^6He}(r) = \rho_0 \exp(-\beta r^2), \quad (22)$$

where β is adjusted to reproduce the experimental value for the rms radius of the ^{6}He=2.54 fm. ρ_0 can be obtained from the normalization condition

$$\int \rho(r) r^2 dr = \frac{A}{4\pi}, \quad (23)$$

where A is the mass number.

4.3. The ^{4}He + ^{6}He + 2n system

Finally, we investigate the ^{4}He + ^{6}He + 2n structure for the ^{12}Be nucleus. For this aim, the density of ^{12}Be is represented in the following form

$$\rho_{^{12}Be}(r) = \rho_{^4He}(r) + \rho_{^6He}(r) + 2\rho_n(r). \quad (24)$$

The ^{4}He and ^{6}He densities used in our analysis are the same as Eq. (18) and Eq. (22), respectively. The density of 1n-halo is in the gaussian form [47, 48]

$$\rho_n(r) = \left(\frac{1}{\gamma\sqrt{\pi}}\right)^3 \exp(-r^2/\gamma^2). \quad (25)$$

4.4. The fitting procedure

In this part, the details of the fitting procedure conducted in the calculations of both the density distributions and internal structure models of ^{12}Be are introduced. In the fitting procedure, a good consistence between the theoretical results and the experimental data of the ^{12}Be + ^{12}C reaction by searching W_0, r_w and a_w parameters of the imaginary potential is tried to obtain. Purely elastic scattering data of the ^{12}Be + ^{12}C reaction are not currently available. Therefore, the quasielastic data instead of the elastic scattering data have been used in the fitting procedure.

We have started from the parameters used in the calculations of the previous studies in the density distribution calculations [13, 14]. In this respect, the values of r_w have been examined in steps from 0.1 to 0.01 fm and have been fixed at 0.90 fm in all the calculations of density distributions. Then, the a_w values have been investigated in steps of 0.1 and 0.001 fm at fixed radius and have been kept constant at 0.905 fm. The fitting procedure of the studied systems has been completed by adjusting the W_0 depth of imaginary potential. The optical potential parameters of all the densities have been listed in Table I.

TABLE I. The optical potential parameters for the VMC, SG, GG, GH, GO and GE densities used in the analysis of the ^{12}Be + ^{12}C system. In all the calculations, the Coulomb radius (R_c) is fixed as 1.25.

Density Distribution	N_R	W (MeV)	r_w (fm)	a_w (fm)	σ (mb)
VMC	0.605	33.4	0.90	0.905	1249.6
SG	0.600	33.9	0.90	0.905	1255.5
GG	0.648	35.0	0.90	0.905	1270.4
GH	0.622	33.5	0.90	0.905	1251.6
GO	0.635	34.5	0.90	0.905	1263.3
GE	0.830	45.6	0.90	0.905	1379.5

TABLE II. The optical potential parameters for the ^{4}He + ^{8}He, ^{6}He + ^{6}He and ^{4}He + ^{6}He + 2n systems used for the ^{12}Be nucleus in the analysis of the ^{12}Be + ^{12}C system. In all the calculations, the Coulomb radius (R_c) are fixed as 1.25.

System	N_R	W (MeV)	r_w (fm)	a_w (fm)	σ (mb)
^{4}He + ^{8}He	0.915	54.0	1.027	0.50	1122.1
^{6}He + ^{6}He	0.855	45.9	1.027	0.50	1087.1
^{4}He + ^{6}He + 2n	1.000	56.0	1.027	0.50	1133.0

Like the analysis of the density distributions, we have tested different values of r_w in steps from 0.1 to 0.001 fm and have fixed the value of r_w at 1.027 fm in all the calculations of the internal structure models. The a_w values have been varied in steps of 0.1 and 0.01 fm at fixed radius and have been kept constant at 0.50 fm. Finally, the fitting procedure of the structure models has been completed by adjusting the W_0 value. The optical potential parameters obtained have been given in Table II.

The code FRESCO [49] has been used in theoretical calculations of the DFM. FRESCO, a general-purpose reaction code, is conducted to generate the OM parameters to fit the data [50].

5. Results and Discussions

The quasielastic scattering of ^{12}Be + ^{12}C system at 679 MeV has been investigated for six different densities of the ^{12}Be nucleus. The densities have been presented in a comparative form in Fig. 1 (logarithmic scale) and Fig. 2 (linear scale). It has been observed that the GE density extends much farther when compared to the other densities. The GG density is longer than the other density distributions except for the GE density. However, the GH and GO densities arrive close

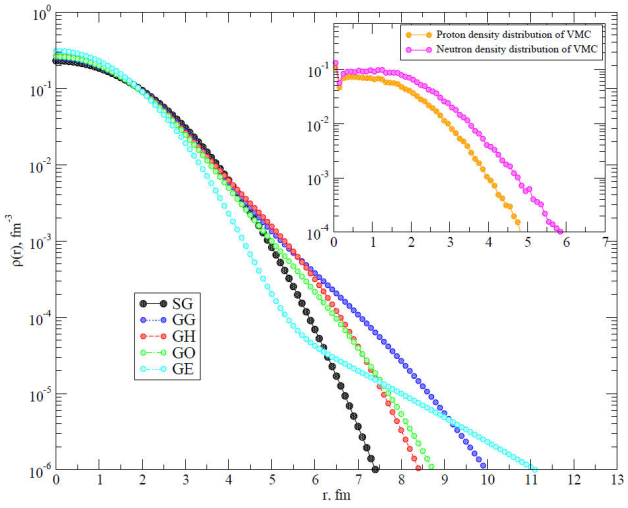

FIGURE 1. The VMC, SG, GG, GH, GO and GE density distributions in logarithmic scale.

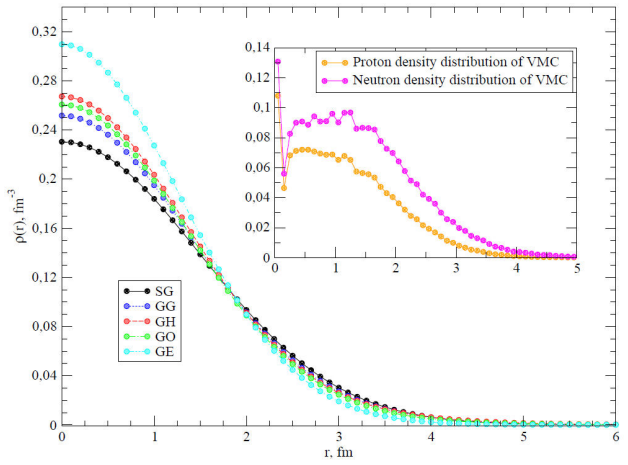

FIGURE 2. Same as Fig. 1, but in linear scale.

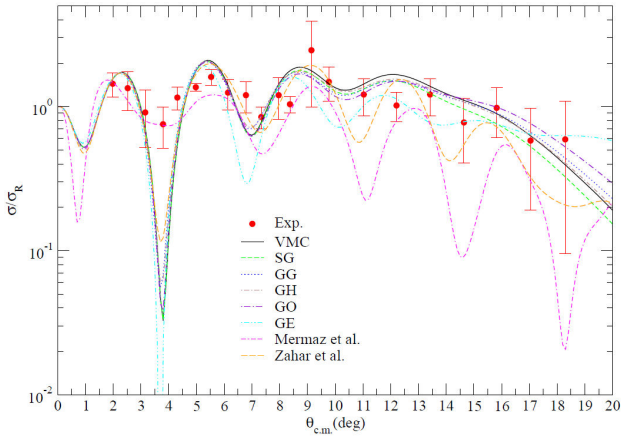

FIGURE 3. The elastic scattering angular distributions for the VMC, SG, GG, GH, GO and GE densities of the ^{12}Be + ^{12}C reaction at E_{Lab}= 679 MeV in comparison with the previous studies [13,14] as well as the experimental data. The experimental data have been taken from [13].

distance with each other, but the GH is shorter. Finally, the SG density is the shortest of all the density distributions.

The theoretical results obtained for different densities have been shown as comparative in Fig. 3. The theoretical results of the density distributions show similar behavior with each other. This similarity breaks down after about $\Theta > 8°$. We have observed that the GE density exhibits a behavior based on the average value of the experimental data compared to the other densities. However, the densities investigated in our study display behavior of the experimental data in general, but none of them is perfect. In addition to this, we compared the theoretical results with the previous works [13, 14] as well as the experimental data in Fig. 3 in order to make a comparative study. While the results of the previous studies [13, 14] have been obtained, we have conducted only the phenomenological calculations for the OM parameters given in Refs. 13 and 14 without including the inelastic scattering of the ^{12}C nucleus. In Refs. 13 and 14, the theoretical results consist of the sum of the elastic and inelastic scattering. Therefore, we should point out that there is some difference between our results and the results of Refs. [13, 14].

Also, we should point out that the normalization constant (N_R), which is used to acquire good consistent results with the experimental data, has been varied. In this respect, the value $N_R = 1.0$ is attributed to the success of the DFM [15]. On the other hand, the deflection from unity of the N_R, the model would mean to need the corrections, denotes strangeness and uncertainties in the data or to uncertainties in the fitting procedures applied or to uncertainties in the densities conducted under the folding model approach [15]. From the parameters given in Table I, the N_R values of all the densities deviates from unity. This result is expected because of including the quasielastic scattering data of the ^{12}Be + ^{12}C system investigated in the present work. However, the deflection from unity of the GE density is less than the other densities.

In our study, we investigated various internal structure models such as the ^{4}He+^{8}He, ^{6}He+^{6}He and ^{4}He+^{6}He+2n

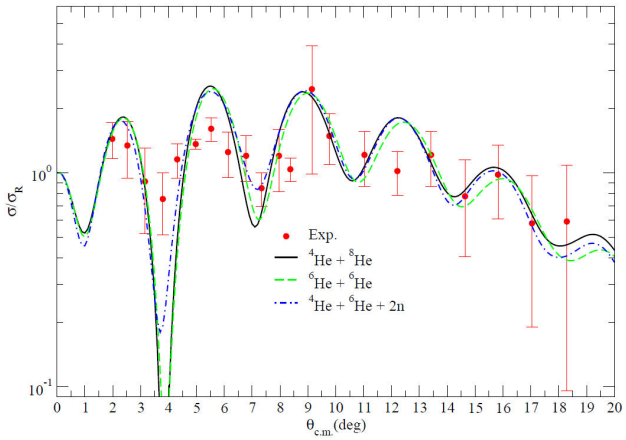

FIGURE 4. The elastic scattering angular distributions for the ^{4}He + ^{8}He, ^{6}He + ^{6}He and ^{4}He + ^{6}He + 2n systems used for the ^{12}Be nucleus in the analysis of the ^{12}Be + ^{12}C system.

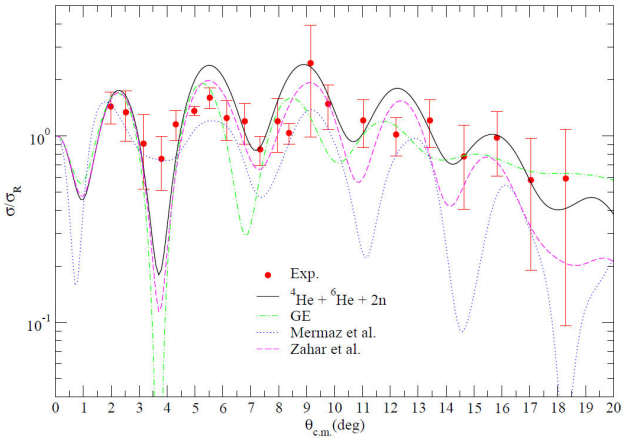

FIGURE 5. A comparison of good consistent elastic scattering results with the experimental data obtained from the density distributions and the structure models used for the ^{12}Be nucleus in the analysis of the ^{12}Be + ^{12}C system.

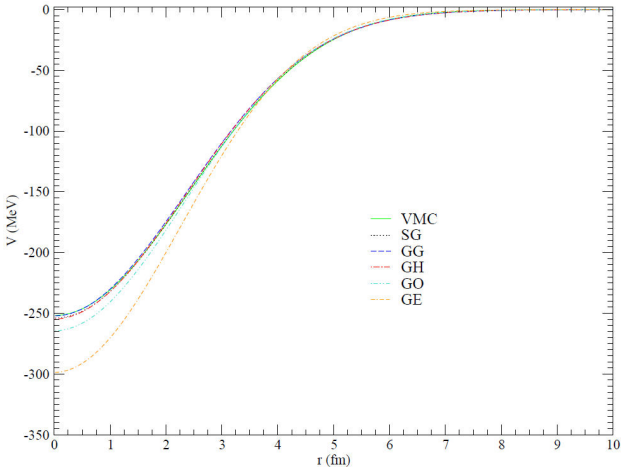

FIGURE 6. The shapes of the real potentials of the nuclear potential of the ^{12}Be + ^{12}C reaction for the VMC, SG, GG, GH, GO and GE densities.

of the ^{12}Be nucleus via a different approach. We obtained the scattering angular distributions of all the models and presented in a comparative manner with each other as well as the experimental data in Fig. 4. We have observed that the results are in very agreement with experimental data. Especially, the ^{4}He + ^{6}He + 2n results are close to the perfection compared to the results of the density distributions investigated in this work. This conclusion is supported with the results of ^{4}He + ^{8}He and ^{6}He + ^{6}He systems. As a result of this, we should say that to investigate the cluster structures of various nuclei by using the method conducted in the present study will be important in the analysis of the nucleus-nucleus interactions.

While the theoretical calculations of the structure models were carried out, the N_R values were changed. If one compares the N_R values applied in the analysis of the density distribution and the internal structure, one can notice that a significant improvement have become in the N_R values of the internal structures. Moreover, ^{4}He + ^{6}He + 2n system has

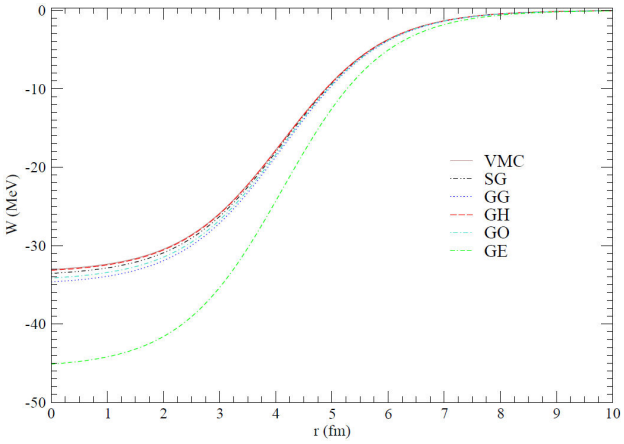

FIGURE 7. The shapes of the imaginary potentials of the nuclear potential of the ^{12}Be + ^{12}C reaction for the VMC, SG, GG, GH, GO and GE densities.

given very agreement results with the data without changing the N_R value. This is another important point of the method conducted in our study.

In Fig. 5, we have compared good agrement results of the analysis of both the density distributions (the GE density) and structure models (^{4}He + ^{6}He + 2n) of the ^{12}Be isotope with the experimental data. It has been clearly seen that the ^{4}He + ^{6}He + 2n model gives very good results compared to the density distribution results and the literature results. As a result of this, we consider that this result would be an important and interesting in the analysis of the ^{12}Be + ^{12}C reaction and the nucleus-nucleus interactions.

In Figs. 6 and 7, the shapes of the real and imaginary potentials conducted for different density distributions of ^{12}Be on the ^{12}C target nucleus have been presented. The real potentials exhibit differences as the depthes. The reason is because different N_R values used for the real potentials. The deepest real potential is seen in the GE density. The other potential depthes are closer with each other. Also, it has been seen that the GE density goes to zero faster than the real potentials of the other densities. When the shapes of the imaginary potential results are examined, it has been observed that the deepest imaginary potential is found for the GE density. The depthes of the other potentials are closer with each other, especially, for the VMC and GH densities. This is because of different W values used in the folding model calculations of the density distributions as given in Table I.

In Figs. 8 and 9, we have shown the shapes of the real and imaginary potentials of the nuclear potential for different internal dynamics of the ^{12}Be nucleus. The real potential of the ^{4}He + ^{8}He system is deeper than the other systems. However, the shallow real potential is attributed to the ^{4}He + ^{6}He + 2n system. If one investigates the behaviors of the imaginary potentials of the systems, one can see that the imaginary potential of the ^{4}He + ^{4}He + 2n system is deeper than the imaginary potentials of other systems. Whereas the shallowest imaginary potential has been found for the ^{6}He + ^{6}He system.

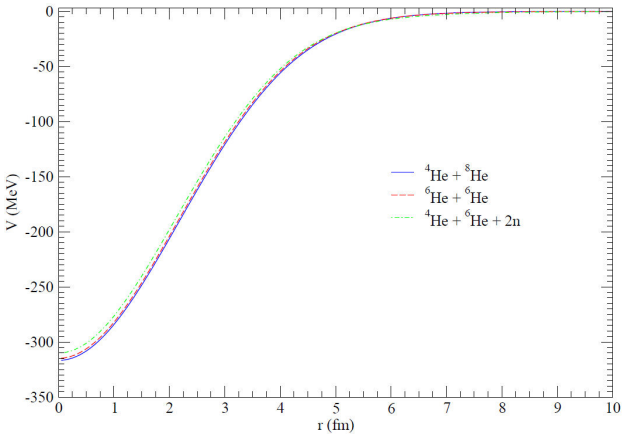

FIGURE 8. The shapes of the real potentials of the nuclear potential of the ^{4}He + ^{8}He, ^{6}He + ^{6}He and ^{4}He + ^{6}He + 2n systems used for the ^{12}Be nucleus in the analysis of the ^{12}Be + ^{12}C system.

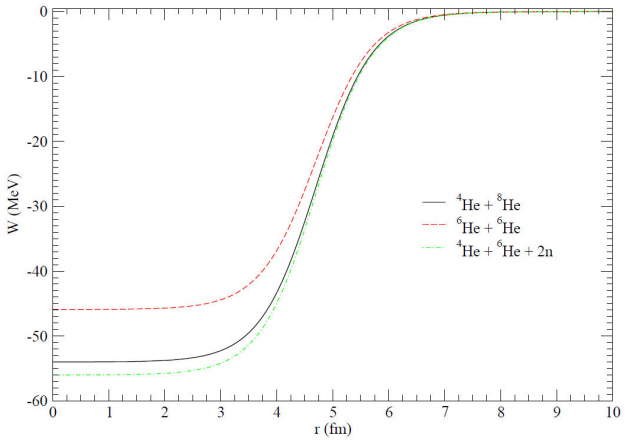

FIGURE 9. The shapes of the imaginary potentials of the nuclear potential of the ^{4}He + ^{8}He, ^{6}He + ^{6}He and ^{4}He + ^{6}He + 2n systems used for the ^{12}Be nucleus in the analysis of the ^{12}Be + ^{12}C system.

In Table I, we have given the cross-sections for all the density distributions which vary in the range of $1249.6 \leq \sigma \leq 1379.5$ mb. Also, in Table II, we have shown the cross-sections in the range of $1087.1 \leq \sigma \leq 1133.0$ mb obtained for various internal structures of the ^{12}Be nucleus. We observed that the cross-sections of the density distributions are bigger than the cross-sections of the structure models. In addition to this, we have compared our results with the cross-sections of the previous studies. In this respect, Zahar [13] reported 1238.0 mb as the value of the cross-section for the ^{12}Be + ^{12}C system. In another study [14], the cross-section for this system was calculated and reported as 911 mb. When our results are compared with the literature results, we can say that the cross-sections obtained by means of different density distributions of the ^{12}Be nucleus are closer to the result of Zahar [13] rather than the cross-sections acquired from other internal structures.

6. Summary and Conclusions

We have performed the theoretical calculations for the elastic scattering of the ^{12}Be + ^{12}C system. We have used six different density distributions for the ^{12}Be nucleus. It can be said that the density distributions define the behavior of the experimental data in general. However, the results need to develop for a perfect consistence with the experimental data. Then, our results have been compared with the literature results. Thus, this work has provided a comprehensive analysis on the validity of six different density distributions of the ^{12}Be nucleus.

In the present work, we have investigated the internal structure models of the ^{12}Be nucleus by using a different approach. In this context, we have analyzed the ^{4}He + ^{8}He, ^{6}He + ^{6}He and ^{4}He + ^{6}He + 2n systems. We have obtained the elastic scattering angular distributions for these systems and have compared our results with the density distribution results as well as the experimental data. The harmony between the theoretical results and the experimental data is quite good. Especially, the results of ^{4}He + ^{6}He + 2n system are in very agreement with the data without renormalization although the experimental data of the ^{12}Be + ^{12}C reaction present a oscillatory behavior. Here, we do not claim very precise results. We are developing a different approach to the analysis of the internal structure of ^{12}Be nucleus based on the DFM. According to the results of this approach, we consider that various structure models of the ^{12}Be nucleus may provide important contributions to the theoretical studies of nucleus-nucleus interactions.

1. Y. Kanada-En'yo, *Phys. Rev. C* **91** (2015) 014315.
2. Z.H. Yang *et al.*, *Phys. Rev. Lett.* **112** (2014) 162501.
3. Z.H. Yang and Y.L. Ye, *Epj Conf.* **66** (2014) 02112.
4. A. Krieger *et al.*, *Phys. Rev. Lett.* **108** (2012) 142501.
5. R. Sherr and H.T. Fortune, *Phys. Rev. C* **60** (1999) 064323.
6. H.T. Fortune, *Phys. Rev. C* **89** (2014) 017302.
7. M. Dufour, P. Descouvemont and F. Nowacki, *Nucl. Phys. A* **836** (2010) 242-255.
8. S. Shimoura *et al.*, *Phys. Lett. B* **560** (2003) 31-36.
9. A. Ozawa, T. Suzuki and I. Tanihata, *Nucl. Phys. A* **693** (2001) 32-62.
10. I. Tanihata, H. Savajols and R. Kanungo, *Prog. Part. Nucl. Phys.* **68** (2013) 215-313.
11. G.D. Alkhazov and V.V. Sarantsev, *Phys. At. Nucl.* **75** (2012) 1544-1549.
12. M.P. Bush, J.S. Al-Khalili, J.A. Tostevin and R.C. Johnson, *Phys. Rev. C* **53** (1996) 3009.

13. M. Zahar *et al.*, *Phys. Rev. C* **49** (1994) 1540.
14. M.C. Mermaz, *Phys. Rev. C* **50** (1994) 2620.
15. G.R. Satchler and W.G. Love, *Phys. Rep.* **55** (1979) 183-254.
16. M. Aygun, Y. Kucuk, I. Boztosun and Awad A. Ibraheem, *Nucl. Phys. A* **848** (2010) 245-259.
17. M. Aygun, *Eur. Phys. J. A* **48** (2012) 145.
18. M. Aygun, I. Boztosun and Y. Sahin, *Phys. At. Nucl.* **75** (2012) 963-968.
19. M. Aygun, I. Boztosun and K. Rusek, *Mod. Phys. Lett. A* **28** (2013) 1350112.
20. M. Aygun, *Ann. Nucl. Energy* **51** (2013) 1-4.
21. M. Aygun, *Commun. Theor. Phys.* **60** (2013) 69-72.
22. M. Aygun and I. Boztosun, *Few-Body Syst.* **55** (2014) 203-209.
23. M. Aygun, O. Kocadag and Y. Sahin, *Rev. Mex. Fis.* **61** (2015) 414-420.
24. F. Hoyle, *Astrophys. J. (Suppl.)* **1** (1954) 12.
25. Z.H. Yang *et al.*, *Phys. Rev. C* **91** (2015) 024304.
26. M. Ito, N. Itagaki, H. Sakurai and K. Ikeda, *Phys. Rev. Lett.* **100** (2008) 182502.
27. Y. Kanada-En'yo, *Physica E* **43** (2011) 811-814.
28. F.M. Nunes, J.A. Christley, I.J. Thompson, R.C. Johnson and V.D. Efros, *Nucl. Phys. A* **609** (1996) 43-73.
29. N. Curtis *et al.*, *Phys. Rev. C* **73** (2006) 057301.
30. Z.H. Yang *et al.*, *Sci. China-Phys. Mech. Astron.* **57** (2014) 1613-1617.
31. A.A. Korsheninnikov *et al.*, *Phys. Lett. B* **343** (1995) 53-58.
32. N.I. Ashwood *et al.*, *Phys. Lett. B* **580** (2004) 129-136.
33. Y. Kanada-En'yo, *Phys. Rev. C* **66** (2002) 011303(R).
34. R.J. Charity *et al.*, *Phys. Rev. C* **76** (2007) 064313.
35. M. Freer *et al.*, *Phys. Rev. C* **63** (2001) 034301.
36. M. Freer *et al.*, *Phys. Rev. Lett.* **82** (1999) 1383.
37. A. Saito *et al.*, *Nucl. Phys. A* **738** (2004) 337-341.
38. P. Descouvemont and D. Baye, *Phys. Lett. B* **505** (2001) 71-74.
39. M. El-Azab Farid and M.A. Hassanain, *Nucl. Phys. A* **678** (2000) 39-75.
40. M. Karakoc and I. Boztosun, *Phys. Rev. C* **73** (2006) 047601.
41. Variational Monte Carlo (VMC) density distribution, http://www.phy.anl.gov/theory/research/density/
42. S. Ilieva, *Investigation of the nuclear-matter density distributions of the exotic* ^{12}Be, ^{14}Be *and* ^{8}B *nuclei by elastic proton scattering in inverse kinematics*, PhD thesis, Johannes Gutenberg-Universität in Mainz, (2008).
43. S. Ilieva *et al.*, *Nucl. Phys. A* **875** (2012) 8-28.
44. G.D. Alkhazov *et al.*, *Nucl. Phys. A* **712** (2002) 269-299.
45. M.V. Zhukov, A.A. Korsheninnikov and M.H. Smedberg, *Phys. Rev. C* **50** (1994) R1.
46. P. Navrátil, W.E. Ormand, E. Caurier and C. Bertulani, UCRL-PROC-211912, Lawrence Livemore National Laboratory (2005).
47. A.K. Chaudhuri, *Phys. Rev. C* **49** (1994) 1603.
48. R.A. Rego, *Nucl. Phys. A* **581** (1995) 119-130.
49. I.J. Thompson, *Computer Phys. Rep.* **7** (1988) 167.
50. M. Aygun, *Acta Phys. Pol. B* **45** (2014) 1875.